

Hyperfine fields in an Ag/Fe multilayer film investigated with ^8Li β -detected NMR

T. A. Keeler,¹ Z. Salman,^{2,*} K. H. Chow,³ B. Heinrich,⁴ M. D. Hossian,¹ B. Kardasz,⁴ R. F. Kiefl,^{1,2} S. R. Kreitzman,² C. D. P. Levy,² W. A. MacFarlane,⁵ O. Mosendz,⁴ T. J. Parolin,⁵ M. R. Pearson,² and D. Wang¹

¹*Department of Physics and Astronomy, University of British Columbia, Vancouver, British Columbia, Canada V6T 1Z1*

²*TRIUMF, 4004 Wesbrook Mall, Vancouver, British Columbia, Canada V6T 2A3*

³*Department of Physics, University of Alberta, Edmonton, Alberta, Canada T6G 2G7*

⁴*Department of Physics, Simon Fraser University, Vancouver, British Columbia, Canada V5A 1S6*

⁵*Department of Chemistry, University of British Columbia, Vancouver, British Columbia, Canada V6T 1Z1*

(Received 12 October 2007; revised manuscript received 2 January 2008; published 28 April 2008)

Low-energy β -detected nuclear magnetic resonance was used to investigate the spatial dependence of the hyperfine magnetic fields induced by Fe in the nonmagnetic Ag of an Au(40 Å)/Ag(200 Å)/Fe(140 Å) (001) magnetic multilayer grown on GaAs. The resonance line shape in the Ag layer shows dramatic broadening compared to that of intrinsic Ag. This broadening is attributed to large magnetic fields induced in this layer by the magnetic Fe layer. We find that the induced hyperfine field in the Ag follows a power law decay away from the Ag/Fe interface with power $-1.93(8)$, and a field extrapolated to 0.23(5) T at the interface.

DOI: [10.1103/PhysRevB.77.144429](https://doi.org/10.1103/PhysRevB.77.144429)

PACS number(s): 75.70.Cn, 76.60.-k, 76.60.Jx

The unique properties exhibited by thin layers of ferromagnetic metal separated by a layer of nonmagnetic metal spacer are both interesting and useful for applications in “spintronic” devices.¹ In these structures the coupling between the ferromagnetic layers oscillates between ferromagnetic (FM) and antiferromagnetic (AF) as a function of the thickness of the nonmagnetic spacer separating them.^{2–5} This interlayer exchange coupling (IEC) is related to an oscillating electronic spin polarization induced in the nonmagnetic spacer due to the magnetic layers. The oscillation period⁶ (~ 10 Å) is governed by the Fermi surface of the metal spacer. While several theoretical models have been developed to explain this behavior, it is difficult to establish which is the most “correct,” since a direct measurement of the effects in the nonmagnetic spacer is challenging. These phenomena led to the discovery of the giant magnetoresistance (GMR) effect,⁷ which is of great scientific interest, and also has important technological ramifications. For example, the drastic increase in hard-disk bit density of the last 20 years was made possible by the vast increase in sensitivity of read heads that incorporate GMR structures. This sensitivity is a consequence of the strong field dependence of the resistivity of GMR structures.

The most well-known model developed to explain the FM-AF coupling oscillations in these systems is an extension of the Ruderman-Kittel-Kasuya-Yosida (RKKY) model describing the effect of a magnetic impurity on the conduction electrons of a nonmagnetic host metal.^{8,9} The oscillations are the result of the sharp cutoff of wave vectors at the Fermi surface in the spacer, resulting in an imperfect screening of the magnetic moments and oscillations in the polarization of conduction electrons. It is via this polarization that the magnetic layers are coupled. The period of oscillation is thus related to the Fermi surface and is determined by the “critical spanning” wave vectors of the spacer material.¹⁰ In Ag there are two critical spanning vectors associated with the “neck” and “belly” regions of the Fermi surface in the (001) direction.

The small amplitude of the induced electronic polariza-

tion (due to rapid decay away from the magnetic layer) as well as the small physical size of typical samples (spacer thicknesses typically several hundred angstroms or less) makes direct measurements of the induced polarization within the nonmagnetic spacer layer very difficult. To date, most quantitative methods used to measure the polarization in the spacer material either are averages of the polarization across the entire spacer, or probe the surface of a nonmagnetic overlayer grown on a ferromagnetic substrate. In particular it is very difficult or impossible to directly probe the spatial dependence of the conduction electron polarization within the nonmagnetic layer. Such measurements require a technique that is sensitive to the local polarization of conduction electrons throughout the entire spacer. Mössbauer spectroscopy,¹¹ perturbed angular correlations,¹² and nuclear orientation¹³ are local probes, but their limited sensitivity restricts them to measurements close to the magnetic-nonmagnetic interface where the induced fields are strongest. In order to probe the behavior deep within the nonmagnetic layer, one requires more sensitive measurements of the local polarization, such as low-energy muon spin rotation (LE μ SR).^{14,15} The technique used herein is depth-resolved β -detected nuclear magnetic resonance (β -NMR).

In this paper we report the results of β -NMR measurements of the induced hyperfine field distribution in the nonmagnetic layer of a Ag(200 Å)/Fe(140 Å) magnetic multilayer (MML) prepared by molecular beam epitaxy (MBE) on a GaAs (001) single-crystal substrate. We find that the induced hyperfine field in the Ag decays away from the Ag/Fe interface following a power law with exponent $\alpha = -1.93(8)$. One of the key parameters in theories describing this effect is the exponent α , which is difficult both to measure and to calculate. However, it has significant fundamental and practical importance since it determines how strongly two magnetic layers separated by a nonmagnetic spacer layer will couple.

β -NMR is a technique closely related to conventional nuclear magnetic resonance. However, in β -NMR the signal is generated using the β -decay properties of highly spin po-

larized radioactive nuclei ($\sim 10^8$) that have been implanted directly into the sample, whereas conventional NMR relies on a much larger number ($\sim 10^{18}$) of intrinsic nuclei to generate a signal. β -NMR experiments conducted in the ISAC facility at TRIUMF use a beam of spin polarized radioactive ^8Li ($I=2$, $\gamma=6301.5$ kHz/T, $\tau=1.21$ s) which is implanted into the sample and used as a spin probe. The ^8Li nuclear polarization, which is the quantity of interest, is monitored through its β decay where a high-energy electron is emitted preferentially opposite to the direction of its nuclear spin. The polarization is measured as a function of the frequency of an applied transverse radio frequency (rf) field. The resulting resonance is a sensitive probe of the local internal electronic and magnetic environment. The implantation energy can be adjusted in the range 0.1–30.5 keV, corresponding to mean implantation depths of between 2 and 200 nm from the sample surface. Previous studies on a Au(40 Å)/Ag(800 Å)/Fe(14 Å) (001) film demonstrated our ability to make depth-resolved β -NMR measurements in the different layers, as well as our sensitivity to the induced hyperfine fields in the Ag close to the Fe.¹⁶ This ability to extract information about the local magnetic environment as a function of depth on a nanometer length scale distinguishes low-energy β -NMR from conventional μSR and NMR. It is similar to $\text{LE}\mu\text{SR}$ in this respect but there are significant differences, e.g., the different time scale, so that the two methods are often complementary. A more complete description of the β -NMR technique can be found elsewhere.^{17,18}

The Au(40 Å)/Ag(200 Å)/Fe(140 Å) MML sample was grown using MBE on a GaAs (001) single-crystal substrate. The substrate was sputtered clean and annealed to yield large flat terraces on which a 140 Å Fe layer was grown. The small lattice mismatch between GaAs and Fe (-1.4%) allows growth of body centered cubic (bcc) Fe (001) into well-ordered layers. Then a 200 Å layer of face centered cubic (fcc) Ag was grown on Fe following the (001) orientation with its lattice rotated by $\pi/4$.¹⁹ The sample was finally capped with a protective 40 Å Au layer. The thicknesses of the layers were monitored during growth using a calibrated quartz crystal microbalance.

The sample was placed in the β -NMR spectrometer in an applied magnetic field of 4.5 T normal to the film surface. Representative β -NMR spectra at room temperature and three different implantation energies are shown in Fig. 1. At full implantation energy (30.5 keV) most of the ^8Li is implanted into the GaAs substrate. The resonance in Fig. 1(a) fits well to a Lorentzian line shape with a width of 4 kHz, as expected for ^8Li in GaAs.²⁰ Figures 1(b) and 1(c) show the spectra obtained with implantation energies 4.0 and 3.5 keV respectively. As shown in Fig. 2, at these energies TRIM.SP Monte Carlo simulations²¹ predict that most of the ^8Li stops in the Ag layer ($\sim 50\%$), with a small amount ($\sim 3\%$) stopping in the Au layer. The remaining ^8Li is backscattered ($\sim 37\%$) or stops in the Fe ($\sim 10\%$). Note, since backscattered ^8Li stops outside the rf coil they do not contribute to the measured resonance line. Similarly, ^8Li stopping in Fe experiences a very large magnetic field and therefore produces a resonance outside our frequency window.²² Recent β -NMR measurements show that the intrinsic ^8Li resonance linewidth in a thin Ag film is 0.5–1 kHz.¹⁸ In contrast, the

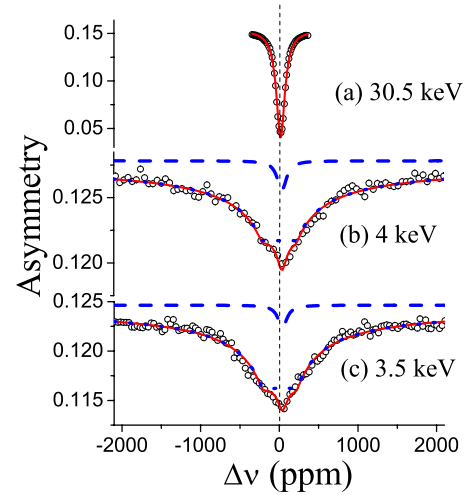


FIG. 1. (Color online) β -NMR spectra measured in the MML sample at room temperature and a field of 4.5 T at implantation energy (a) 30.5, (b) 4, and (c) 3.5 keV. The solid red lines are best fits to the calculated line shapes (see text). The dotted and dashed lines represent the contributions from ^8Li in Ag and Au, respectively.

linewidth observed in Figs. 1(b) and 1(c) is an order of magnitude larger. This broadening is attributed to the induced hyperfine magnetic field in Ag due to the Fe magnetic layer.

We now discuss the modeling of the line shapes obtained, such as those shown in Fig. 1. Following the RKKY-based theoretical description,²³ the induced hyperfine field in Ag as a function of the distance (x) from an ideal Ag/Fe interface, follows

$$B(x) = \sum_{i=0}^1 B_i \left(\frac{x}{\lambda_i} \right)^{\alpha_i} \sin \left(\frac{2\pi x}{\lambda_i} + \phi_i \right), \quad (1)$$

where $\lambda_i = 2\pi/k_i$ are the Fermi wavelengths associated with the two critical spanning vectors, i.e., the belly and neck. The expected resonance line shape, representing the magnetic field probability distribution for the implanted ^8Li , is calculated using Eq. (1), and the stopping ^8Li profile in the Ag layer determined using TRIM.SP calculations (Fig. 3). An ex-

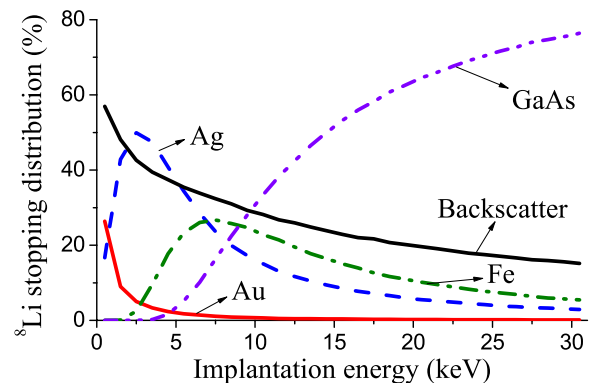


FIG. 2. (Color online) Percentage of ^8Li stopping in each layer of the MML sample as a function of implantation energy, calculated using TRIM.SP Monte Carlo simulation.

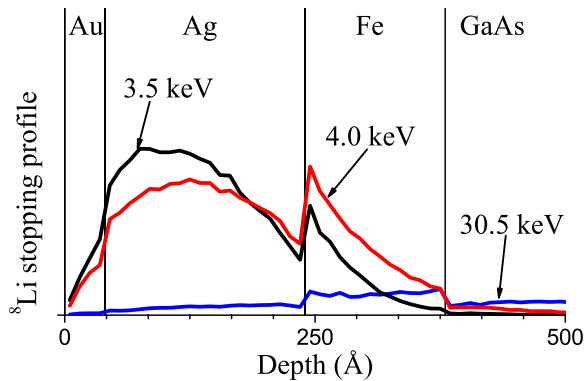


FIG. 3. (Color online) ^8Li stopping profile in the MML sample generated using TRIM.SP Monte Carlo simulations for implantation energies of 3.5, 4.0, and 30.5 keV. At lower energies ^8Li stops predominantly in the Ag layer, while at the full energy nearly all ^8Li stops in the GaAs substrate.

ample calculated using Eq. (1), with a contribution only from the belly-spanning vector ($\lambda = 11.7 \text{ \AA}$), is shown in Fig. 4(a). The contribution from the neck-spanning vector is negligible, since its associated wavelength ($\sim 4.85 \text{ \AA}$) is on the same length scale as the minimum distance between neighboring ^8Li stopping sites, and hence its contribution is averaged out over the ^8Li stopping sites in the Ag lattice. The distinguishing features of this line shape are the peaks on either side of the applied field (B_{ext}) resulting from Van Hove singularities. The large inner double peaks result from the nonzero hyperfine fields at the Ag farthest from the Ag/Fe interface. However, it has been shown that even slight interface roughness tends to wipe out the short-wavelength oscillations in the electron polarization²⁴ since the distance to the interface no longer has a well-defined value over lateral distances larger than the terrace width. Furthermore a vertical mismatch between atomic planes, as little as 0.8% for Ag/Fe(001), also leads to suppression of both the long and short wavelengths.²⁵ The ^8Li beam averages over the area of the beam spot ($\sim 3 \text{ mm}$ diameter); therefore we do not expect to observe oscillations of the induced hyperfine fields. This will have the effect of smearing out the oscillations in the induced field [Eq. (1)]. Therefore we use a phenomenological form for the induced field distribution:

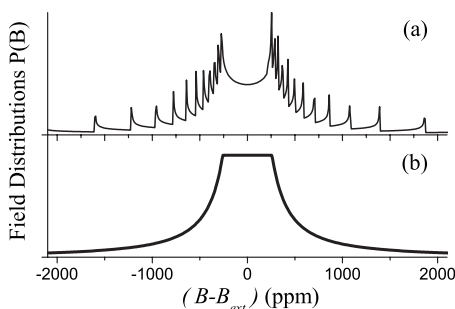


FIG. 4. Simulated line shape, in an applied field B_{ext} , generated for induced hyperfine fields that follows (a) an oscillating distribution described by Eq. (1) and (b) a uniform distribution within the envelope described by Eq. (2). Both line shapes were calculated using $\lambda = 11.7 \text{ \AA}$, $\alpha = -1.9$, $B_0 = 0.23 \text{ T}$, and $B_{\text{ext}} = 4.5 \text{ T}$.

$$B_{\text{max}}(x) = \frac{B_0}{1 + (\lambda_F/x)^\alpha}, \quad (2)$$

with $\lambda_F = 2\pi/k_F$ taken as the long-period Fermi wavelength of Ag (11.7 \AA). We assume that at a particular distance x from the interface, the hyperfine field is equally likely²⁶ to have any value in the range $B_{\text{ext}} \pm B_{\text{max}}(x)$. This form has several advantages: (1) it gives a value of B_0 for the hyperfine field right at the Ag/Fe interface, (2) it maintains the asymptotic power law behavior x^α predicted by RKKY, and (3) it avoids the unphysical divergent behavior at the Ag/Fe interface in Eq. (1). The line shape, shown in Fig. 4(b), results from this form of field distribution. Note that it does not have the peaks associated with the oscillating magnetic field, but it is symmetric and exhibits a characteristic flat top. This low-field cutoff originates from the fact that the hyperfine field does not decay to zero at the Ag/Au interface. This line shape is consistent with the β -NMR spectra in Figs. 1(a) and 1(b).

Note that, in contrast to the calculation above and the line shape in Fig. 4(b), the experimental β -NMR spectra show a sharp peak and not a flat top feature. This is attributed to the small amount of ^8Li that stops in the thin Au capping layer [dashed lines in Fig. 1(b) and 1(c)]. These spectra were fitted to the sum of our model line shape, Fig. 4(b), and a Lorentzian to account for the small signal from Au. The contributions to the measured resonances from Ag and Au, as obtained from the fit, are represented by the dotted and dashed lines in Fig. 1, respectively. The induced field parameters extracted from the fits in Figs. 1(b) and 1(c) are $\alpha = -1.93(8)$ and $B_0 = 0.23(5) \text{ T}$ (common for both spectra). The Lorentzian fit for the resonance in Au was found to be $\sim 4 \text{ kHz}$ wide, and shifted approximately +40 parts per million (ppm) relative to the GaAs reference. The Knight shift of the Au is comparable with previous measurements of intrinsic Au [$+60(20) \text{ ppm}$],²⁷ but the width is about twice that of previous measurements. This may be due to the higher rf power used in these experiments but could also be due to the induced fields from Fe extending into the Au layer. In addition, we find that the ratio of the contribution from Au to Ag from the fit parameters (i.e., the ratio of the areas of the resonance in Au to that in Ag) is $\sim 3\%$, in reasonable agreement with $\sim 6\%$ from TRIM.SP calculations (Fig. 2). The 3% difference may be due to the limited accuracy of TRIM.SP in predicting ion implantation profiles, especially at low implantation energies.^{21,28}

The extracted value of $B_0 = 0.23(5) \text{ T}$, which is the hyperfine coupling of ^8Li at the Ag/Fe interface, is in reasonable agreement with the calculated value 0.30 T for the induced hyperfine field at the first Ag layer at the interface.²⁹ Also, the asymptotic power of the induced field, $\alpha = -1.93(8)$, agrees very well with the theoretical value -2 predicted by RKKY theory.^{23,24,30} It is, however, larger than the values $\alpha = -0.4(1)$ and $-0.8(1)$ measured using LE μ SR in Fe(40 \AA)/Ag(3000 \AA)(001) (Ref. 14) and Fe(40 \AA)/Ag(200 \AA)/Fe(40 \AA)(001) (Ref. 15) samples, respectively. Similarly, using Cu NMR to measure the spin polarization profile in multilayers of Ni/Cu, Goto *et al.*³¹ found $\alpha = -1$. In all those measurements, induced fields of the form Eq. (1) were as-

sumed, and a magnetic field parallel to the surface was used to perform these measurements, while in our measurements the field was applied perpendicular to the surface. In principle, this should not affect the value of α .³¹ The source of discrepancy between our results and those from Refs. 14, 15, and 31 may be the reduced sensitivity of the previous measurements to the interface region. In the LE μ SR measurements, the contribution of the 3 nm region of the Ag/Fe interface is negligible,¹⁴ since the muons in this region experience a field that is too high to be measured. Note that both NMR and LE μ SR measurements are performed in the time domain, i.e., the high-field contribution occurs at early times; therefore the dead time associated with the measurement decreases the sensitivity to high-field regions (interface). In contrast, our measurements are performed directly in the frequency domain and therefore have no such effect (provided that one sweeps a sufficiently large frequency range). In addition, in NMR measurements it is extremely hard to account for the contribution of all nuclei in the spacer since the resonance cannot be normalized, while the method of detection used in β -NMR enables detection of the signal from all implanted spin probe nuclei. Finally, we would like to point out that calculation based on the quantum-interference model³²

predict an oscillating polarization that involves three terms with $\alpha = -1, -2,$ and -3 . Thus, it may be that the different techniques are sensitive to different terms.

In conclusion, we have carried out depth-resolved low-energy ^8Li β -NMR to measure directly the hyperfine field profile in an Ag layer induced by a magnetic Fe layer. No indication of an oscillating hyperfine field is observed. However, we find that the induced fields decrease away from the Ag/Fe interface, following an asymptotic power law $x^{-1.93(8)}$, in good agreement with theoretical calculations based on RKKY theory. The induced field at the Ag/Fe interface $B_0 = 0.23(5)$ T is also in good agreement with calculations.

This research was supported by the Center for Materials and Molecular Research at TRIUMF, the Natural Sciences and Engineering Research Council of Canada, and the Canadian Institute for Advanced Research. We would like to thank W. Eckstein from MPI für Plasmaphysik in Garching, Germany, who developed the TRIM.SP code we used to generate the stopping profiles. We would especially like to thank Rahim Abasalti, Bassam Hitti, and Donald Arseneau for their expert technical support.

*Present address: Clarendon Laboratory, Department of Physics, Oxford University, Parks Road, Oxford OX1 3PU, U.K. z.salman1@physics.ox.ac.uk

¹B. Heinrich and J. F. Cochran, *Adv. Phys.* **42**, 523 (1993).

²P. Grunberg, R. Schreiber, Y. Pang, M. B. Brodsky, and H. Sowers, *Phys. Rev. Lett.* **57**, 2442 (1986).

³B. Heinrich, Z. Celinski, J. F. Cochran, W. B. Muir, J. Rudd, Q. M. Zhong, A. S. Arrott, K. Myrtle, and J. Kirschner, *Phys. Rev. Lett.* **64**, 673 (1990).

⁴S. S. P. Parkin, N. More, and K. P. Roche, *Phys. Rev. Lett.* **64**, 2304 (1990).

⁵S. S. P. Parkin and D. Mauri, *Phys. Rev. B* **44**, 7131 (1991).

⁶S. S. P. Parkin, *Phys. Rev. Lett.* **67**, 3598 (1991).

⁷IEC is generally not a necessary condition for observing the GMR effect. However, if one does not have a spin-valve structure, an antiferromagnetic coupling is necessary to observe the GMR effect.

⁸D. M. Edwards, J. Mathon, R. B. Muniz, and M. S. Phan, *Phys. Rev. Lett.* **67**, 493 (1991).

⁹P. Bruno and C. Chappert, *Phys. Rev. B* **46**, 261 (1992).

¹⁰M. D. Stiles, *J. Magn. Magn. Mater.* **200**, 322 (1999).

¹¹Y. Kobayashi, S. Nasu, T. Emoto, and T. Shino, *Hyperfine Interact.* **111**, 129 (1998).

¹²B.-U. Runge, M. Dippel, G. Fillebock, K. Jacobs, U. Kohl, and G. Schatz, *Phys. Rev. Lett.* **79**, 3054 (1997).

¹³T. Phalet, M. J. Prandolini, W. D. Brewer, P. Schuurmans, N. Severijns, B. G. Turrell, B. Vereecke, and S. Versyck, *Phys. Rev. B* **71**, 144431 (2005).

¹⁴H. Luetkens, J. Korecki, E. Morenzoni, T. Prokscha, A. Suter, M. Birke, N. Garifanov, R. Khasanov, T. Slezak, and F. J. Litterst, *J. Magn. Magn. Mater.* **272–276**, 1128 (2004).

¹⁵H. Luetkens, J. Korecki, E. Morenzoni, T. Prokscha, M. Birke,

H. Gluckler, R. Khasanov, H.-H. Klauss, T. Slezak, A. Suter, E. M. Forgan, Ch. Niedermayer, and F. J. Litterst, *Phys. Rev. Lett.* **91**, 017204 (2003).

¹⁶T. A. Keeler, Z. Salman, K. H. Chow, B. Heinrich, M. D. Hossain, B. Kardasz, R. F. Kiefl, S. R. Kreitzman, W. A. MacFarlane, and O. Mosendz, *Physica B* **374–375**, 79 (2006).

¹⁷R. F. Kiefl *et al.*, *Physica B* **326**, 189 (2003); Z. Salman, E. P. Reynard, W. A. MacFarlane, K. H. Chow, J. Chakhalian, S. R. Kreitzman, S. Daviel, C. D. P. Levy, R. Poutissou, and R. F. Kiefl, *Phys. Rev. B* **70**, 104404 (2004); Z. Salman, R. F. Kiefl, K. H. Chow, M. D. Hossain, T. A. Keeler, S. R. Kreitzman, C. D. P. Levy, R. I. Miller, T. J. Parolin, M. R. Pearson, H. Saadaoui, J. D. Schultz, M. Smadella, D. Wang, and W. A. MacFarlane, *Phys. Rev. Lett.* **96**, 147601 (2006); T. J. Parolin, Z. Salman, J. Chakhalian, Q. Song, K. H. Chow, M. D. Hossain, T. A. Keeler, R. F. Kiefl, S. R. Kreitzman, C. D. P. Levy, R. I. Miller, G. D. Morris, M. R. Pearson, H. Saadaoui, D. Wang, and W. A. MacFarlane, *ibid.* **98**, 047601 (2007); Z. Salman, A. I. Mansour, K. H. Chow, M. Beaudoin, I. Fan, J. Jung, T. A. Keeler, R. F. Kiefl, C. D. P. Levy, R. C. Ma, G. D. Morris, T. J. Parolin, D. Wang, and W. A. MacFarlane, *Phys. Rev. B* **75**, 073405 (2007); Z. Salman, D. Wang, K. H. Chow, M. D. Hossain, S. Kreitzman, T. A. Keeler, C. D. P. Levy, W. A. MacFarlane, R. I. Miller, G. D. Morris, T. J. Parolin, H. Saadaoui, M. Smadella, and R. F. Kiefl, *Phys. Rev. Lett.* **98**, 167001 (2007); Z. Salman, K. H. Chow, R. I. Miller, A. Morrello, T. J. Parolin, M. D. Hossain, T. A. Keeler, C. D. P. Levy, W. A. MacFarlane, G. D. Morris, H. Saadaoui, D. Wang, R. Sessoli, G. G. Condorelli, and R. F. Kiefl, *Nano Lett.* **7**, 1551 (2007).

¹⁸G. D. Morris, W. A. MacFarlane, K. H. Chow, Z. Salman, D. J. Arseneau, S. Daviel, A. Hatakeyama, S. R. Kreitzman, C. D. P.

- Levy, R. Poutissou, R. H. Heffner, J. E. Elenewski, L. H. Greene, and R. H. Kiefl, *Phys. Rev. Lett.* **93**, 157601 (2004).
- ¹⁹P. Etienne, J. Massies, F. Nguyen-Van-Dau, A. Barthelemy, and A. Fert, *Appl. Phys. Lett.* **55**(21), 2239 (1989).
- ²⁰K. H. Chow, Z. Salman, W. A. MacFarlane, B. Campbell, T. A. Keeler, R. F. Kiefl, C. D. P. Levy, G. D. Morris, T. J. Parolin, R. Poutissou and Z. Yamani, *Physica B* **374-375**, 415 (2006).
- ²¹W. Eckstein, *Computer Simulation of Ion-Solid Interactions* (Springer, Berlin, 1991).
- ²²K. Matsuta, M. Sasaki, T. Tsubota, S. Kaminaka, S. Kudo, M. Ogura, K. Arimura, M. Mihara, M. Fukuda, H. Akai, and T. Minamisono, *Hyperfine Interact.* **136**, 379 (2001).
- ²³P. Bruno and C. Chappert, *Phys. Rev. Lett.* **67**, 1602 (1991).
- ²⁴Y. Wang, P. M. Levy, and J. L. Fry, *Phys. Rev. Lett.* **65**, 2732 (1990).
- ²⁵Z. Celinski and B. Heinrich, *J. Magn. Magn. Mater.* **99**, L25 (1991); B. Heinrich, Z. Celinski, J. F. Cochran, A. S. Arrott, K. Myrtle, and S. T. Purcell, *Phys. Rev. B* **47**, 5077 (1993).
- ²⁶Models where increased weight is given to the extremal regions ($B_{\text{ext}} \pm B_{\text{max}}$) were also considered. However, the fitting parameters and line shapes produced were very similar to those obtained using the simpler model. Therefore we used the simpler model to analyze our results.
- ²⁷W. A. MacFarlane, G. D. Morris, T. R. Beals, K. H. Chow, R. A. Baartman, S. Daviel, S. R. Dunsiger, A. Hatakeyama, S. R. Kreitzman, C. D. P. Levy, R. I. Miller, K. M. Nichol, R. Poutissou, and R. F. Kiefl, *Physica B* **326**, 213 (2003).
- ²⁸E. Morenzoni, H. Glucker, T. Prokscha, R. Khasanov, H. Luetkens, M. Birke, E. M. Forgan, C. Niedermayer, and M. Pleines, *Nucl. Instrum. Methods Phys. Res. B* **192**, 254 (2002).
- ²⁹C. O. Rodriguez, M. V. Ganduglia-Pirovana, E. L. Peltzer y Blancá, M. Petersen, and P. Novák, *Phys. Rev. B* **63**, 184413 (2001).
- ³⁰Y. Yafet, *Phys. Rev. B* **36**, 3948 (1987).
- ³¹A. Goto, H. Yasuoka, H. Yamamoto, and T. Shinjo, *J. Phys. Soc. Jpn.* **62**, 2129 (1993).
- ³²K. Ishiji, H. Hashizume, Y. Suzuki, and E. Tamura, *Phys. Rev. B* **74**, 174432 (2006).